Journal of Power Sources 209 (2012) 295–300

Contents lists available at SciVerse ScienceDirect

Journal of Power Sources

journal homepage: www.elsevier.com/locate/jpowsour

Electrochemical performances of two kinds of electrolytes based on lithium bis(oxalate)borate and sulfolane for advanced lithium ion batteries

Shiyou Li, Bucheng Li, Xiaoli Xu, Xinming Shi, Yangyu Zhao, Liping Mao, Xiaoling Cui*

College of Petrochemical Technology, Lanzhou University of Technology, Lanzhou 730050, China

ARTICLE INFO

Article history:
Received 25 November 2011
Received in revised form 1 March 2012
Accepted 2 March 2012
Available online 7 March 2012

Keywords:
Lithium ion batteries
Sulfolane
Sulfite
Lithium bis(oxalate)borate

ABSTRACT

Lithium bis(oxalato)borate (LiBOB) is a promising salt for lithium ion batteries. However, to achieve better electrochemical performance of LiBOB, the development of appropriate electrolytes is essential. In this work, the electrochemical behaviors of sulfolane (SL) with LiBOB were studied by employment of dimethyl sulfite (DMS) and diethyl sulfite (DES) as mixed solvents, respectively. Both of the LiBOB-based electrolytes show high oxidation potentials (>5.5 V), and good conductivities. When used in Li/MCMB (mesophase carbon microbeads) cells, these two kinds of novel electrolytes exhibit not only excellent film-forming characteristics, but also low impedances of the interface films. Besides, when used in $LiFePO_4$/Li cells, compared to the cell with the electrolyte system of 1 M $LiPF_6$-EC/DMC (1:1, v/v), both of the LiBOB-based electrolytes exhibit several advantages, such as more stable cycle performance even at elevated temperature, and higher mean voltage.

1. Introduction

The electrolyte for commercial lithium ion battery is usually composed of $LiPF_6$ salt dissolved in a mixture of ethylene carbonate (EC) and linear esters, such as dimethyl carbonate (DMC), diethyl carbonate (DEC), and ethyl methyl carbonate (EMC). It has some unique balance of properties, such as good ionic conductivity and ability to passivate an aluminum current collector. However, $LiPF_6$ is thermally unstable and easy to decompose into undesired products as LiF and PF_5. The formed PF_5 gas is a very strong Lewis acid and easily reacts with organic solvents or solid electrolyte interface (SEI) components in lithium ion batteries [1–3]. Therefore, the search for alternative salts and solvents for lithium ion batteries has received increasing attention lately.

Due to its high solubility in organic solvents, low toxicity, high thermal and electrochemical stability [4–8], lithium bis(oxalato)borate (LiBOB) has attracted much attention as a lithium salt or an additive in nonaqueous electrolytes for lithium ion batteries. However, LiBOB has low solubility and inferior conductivity in alkyl carbonate solvents. In addition, when used in cells, the formation of the SEI layer on the surface of carbonaceous anode materials has high impedance to harm the cryogenic property and discharge capacity of batteries [9,10]. Therefore, to improve the electrochemical performance of LiBOB, the exploring of appropriate electrolytes and applying them to lithium ion batteries is of special interest.

Generally, to obtain suitable properties of an electrolyte, the common approach is to mix a solvent having high dielectric constant and high viscosity with other solvents having low relative permittivity and low viscosity [11]. Sulfolane (SL) is a common solvent known to have high dielectric constant, boiling point and flash point. However, SL is in solid state at room temperature, and its viscosity is high in liquid phase. So, in this study, dimethyl sulfite (DMS) and diethyl sulfite (DES) were respectively chosen to realize advantage complementation. Some important physical properties of these solvents are listed in Table 1.

This report is focused on the investigation of the electrochemical performances of these two kinds of novel electrolytes, LiBOB-SL/DMS and LiBOB-SL/DES, to seek the promising candidate for advanced lithium-ion batteries.

2. Experimental

LiBOB was synthesized in our laboratory by employing a solid-state reaction [12,13], and purified to above 99.8% by repeating recrystallizations with anhydrous CH_3CN several times. Organic sulfites DMS and DES were synthesized according to the methods available in the literature [14]. SL was obtained from Liaoyang Guanghua Chemical Co., Ltd. Each kind of solvents was dried by 0.4 nm molecular sieves and alkali metal for at least two days until the water content was typically less than 1×10^{-6} mg L^{-1} determined by Karl Fischer titration.

* Corresponding author. Tel.:+86 931 2973305; fax: +86 931 2973648.
E-mail address: sylilw@163.com (X. Cui).

0378-7753/$ – see front matter.
doi:10.1016/j.jpowsour.2012.03.004

Table 1
Some important physical properties of the solvents.

Solvents	Melting point (°C)	Boiling point (°C)	Flash point (°C)	Dielectric constant	Viscosity (mPa S)
Sulfolane	28.5	285	166	43.3	10.2
Ethylene carbonate	39.6	248	160	89.6	0.18
Dimethyl sulfite	−141	126	30	22.5	0.87
Diethyl sulfite	−112	159	53	15.6	0.83
Dimethyl carbonate	4.6	90	18.3	3.1	0.58

1.0 M $LiPF_6$-EC/DMC (1:1, v/v, the same as follows), which was used as a control electrolyte, was purchased from Zhangjiagang Guotai-Huarong New Chemical Materials Co., Ltd. Two kinds of novel electrolytes, 0.7 M LiBOB-SL/DMS (1:1) and 0.7 M LiBOB-SL/DES (1:1), were prepared in an argon atmosphere glove box.

The electrochemistry windows was measured in a three-electrode system (a planar carbon was used as working electrode, and lithium sheet was used both as counter electrode and reference electrode) for the cyclic voltammetry (CV) at the scanning rate of 2 mV s^{-1} in the range of 3.0–6.5 V.

The ionic conductivities of the electrolytes were measured by DDSJ-308A conductivity meter (Shanghai China) over a temperature range of −30 °C to 60 °C.

The positive electrode was composed of 75 wt.% $LiFePO_4$, 10 wt.% polyvinylidene fluoride (PVDF) and 15 wt.% carbon black. The negative electrode was composed of 92 wt.% mesophase carbon microbeads (MCMB) and 8 wt.% PVDF.

Electrochemical impedance spectroscopy (EIS) spectra of the negative electrode were measured in a three-electrode cell (the negative electrode was used as working electrode with the reaction area of 1 cm^2, and lithium sheet was used both as counter electrode and reference electrode) through CHI660C electrochemical analyzer (Shanghai, China). A sinusoidal AC perturbation of 5 mV was applied to the electrode over the frequency range of 100 kHz to 10 mHz.

Experimental cells were assembled in an argon atmosphere glove box using lithium sheet as anode, the above prepared electrode as cathode, 0.7 M LiBOB-SL/DMS, 0.7 M LiBOB-SL/DES, or 1.0 M $LiPF_6$-EC/DMC as electrolyte, and a Celgard (2400) porous polypropylene as separator. Cells' electrochemical properties tests were carried out on land celltester CT2001A (Wuhan, China) in the different voltage range of 0.003–2 V for Li/MCMB cells, and 2.7–4.2 V for $LiFePO_4$/Li cells.

3. Results and discussion

3.1. Electrochemical stabilities of the three electrolytes

The electrochemical stabilities of the three electrolytes were investigated by CV. The results are shown in Fig. 1. It indicates that the electrochemical stabilities of LiBOB-SL/DMS and LiBOB-SL/DES electrolytes are higher than that of $LiPF_6$-EC/DMC. The current density of $LiPF_6$-EC/DMC electrolyte starts to increase dramatically when the potential is higher than 4.8 V, while the current densities of both of the novel LiBOB-SL/DMS and LiBOB-SL/DES electrolytes increase more slowly and are always lower than that of the $LiPF_6$-EC/DMC, respectively. The oxidation potentials of both of the LiBOB-based electrolytes are higher than 5.5 V. It is obvious that the electrochemical stabilities of both of the LiBOB-SL/DMS and LiBOB-SL/DES electrolytes are sufficient. The results also show that these two kinds of novel electrolytes would be alternative electrolytes for 5 V high-voltage lithium ion batteries.

3.2. Conductivity measurements

Conductivities of the three kinds of electrolytes were measured from −30 °C to 60 °C. The results are shown in Fig. 2. It is obvious that, from −20 °C to 60 °C, conductivities of LiBOB-SL/DMS and LiBOB-SL/DES are lower than that of $LiPF_6$-EC/DMC, especially at high temperature, though both of them are all high enough to be used in lithium ion batteries. The low conductivity is mainly due to the high viscosity constant of SL. However, low temperature performance of $LiPF_6$-EC/DMC is poorer than that of LiBOB-SL/DMS or LiBOB-SL/DES, respectively. Trace of solid material emerges from the $LiPF_6$-EC/DMC electrolyte just at −20 °C, and more and more precipitation is produced with the decrease of the temperature. At −30 °C, $LiPF_6$-based electrolyte solution fully changes to a solid state, owing to EC and DMC having higher melting points than SL and DMS or DES, respectively.

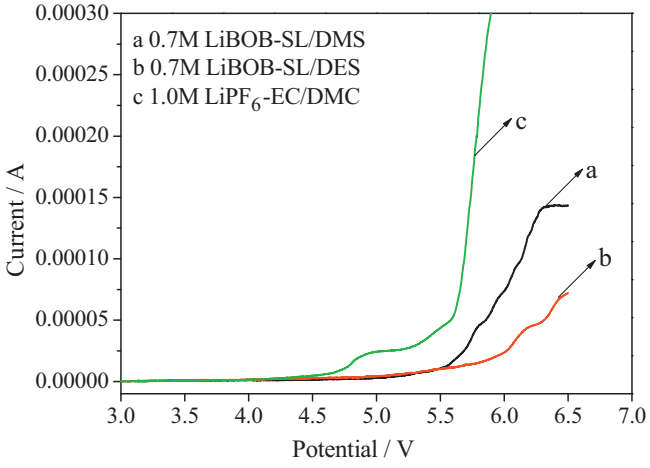

Fig. 1. Current–potential curves of different electrolytes at a scan rate of 2 mV s^{-1} in the range of 3.0–6.5 V at room temperature.

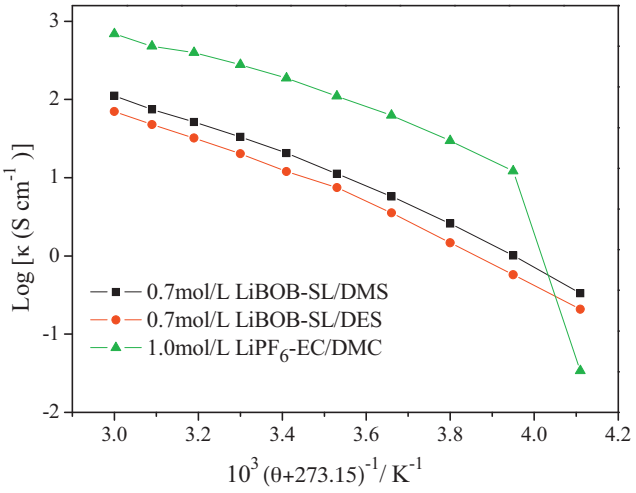

Fig. 2. The dependence of ionic conductivity on temperature for three kinds of electrolytes.

Table 2
Fitting parameters of Arrhenius Equation to the temperature-dependent conductivities of three kinds of electrolytes.

Electrolytes	Temperature range	E_k (J mol^{-1})	r
LiBOB-SL/DMS	−30 to 60 °C	1.85 e4	0.9949
LiBOB-SL/DES	−30 to 60 °C	1.87 e4	0.9952
$LiPF_6$-EC/DMC	−20 to 60 °C	1.49 e4	0.9909

Moreover, Arrhenius Eq. (1) was used to investigate the change law of conductivity κ (with the unit of ms cm^{-1}) with temperature θ (with the unit of K) over the temperature range from −30 °C to 60 °C for two kinds of LiBOB-based electrolytes, and over the temperature range from −20 °C to 60 °C for $LiPF_6$-EC/DMC electrolyte, respectively.

$$\kappa = A \exp\left[-\frac{E_\kappa}{R(\theta + 273.15)}\right], \quad (1)$$

where A is a constant, R is the molar gas constant ($R = 8.314$ J mol^{-1} K^{-1}), E_k is the conductometric apparent activation energy with the unit of J mol^{-1}.

As for Arrhenius equation, when construct the curve of $\ln\kappa$ with $1/(\theta + 273.15)$, a line can be obtained with the slope value of $-E_a/R$. The fitting parameters are showed in Table 2. If $r \geq 0.990$ is taken as the boundary, the results show that the change law is in agreement with Arrhenius equation for each of the above three kinds of electrolytes. It is therefore suggested that there is some thermally activated, diffusion process responsible for the changes in resistance vs. temperature.

3.3. Electrochemical characteristics of the first cycle of Li/MCMB cells

The first charge and discharge curves of Li/MCMB half cells with different electrolyte system are given in Fig. 3a. It is obvious that there are three plateaus in every electrolyte system. The first plateau is presented at about 1.8–1.5 V for LiBOB-based cells and 1.4–1.2 V for $LiPF_6$-based cell, respectively. Correspondingly, 1.6 V reductive peak of LiBOB-SL/DMS, 1.7 V reductive peak of LiBOB-SL/DES, and 1.3 V reductive peak of $LiPF_6$-EC/DMC are given in Fig. 3b. The peak areas of both of the LiBOB-based cells are obviously larger than $LiPF_6$-based cell, respectively. For example, the percentage integral area of cell with LiBOB-SL/DMS electrolyte system is about 10.8%, but the percentage integral area of cell with $LiPF_6$-EC/DMC electrolyte system is only about 4.3%. The reason is that, the reductive peaks of LiBOB-based cells arise from the reduction of BOB anion which plays an active role in the formation of a preliminary unstable SEI layer [15,16], while the reductive peak of $LiPF_6$-based cell is associated with little inserted EC. The second plateau is respectively presented at about 0.8–0.5 V in every electrolyte system, that is associated with the irreversible reduction of both electrolyte components and surface chemical groups of graphite, and the resulting SEI layer is structurally compact and stable [10,17]. Correspondingly, 0.55 V reductive peak of LiBOB-SL/DMS, 0.65 V reductive peak of LiBOB-SL/DES, and 0.52 V reductive peak of $LiPF_6$-EC/DMC, which are also given in Fig. 3b. The prior two plateaus or peaks can be apparently observed only in the first graphite–lithiation cycle due to the self-limiting nature of SEI layer growth on graphite. The well-known intercalation of Li^+ ions into graphite occurs below 0.3 V, which is associated with the third plateau in Fig. 3a and the end of the elevation in Fig. 3b. This process has good reproducibility in the subsequent cycles [18].

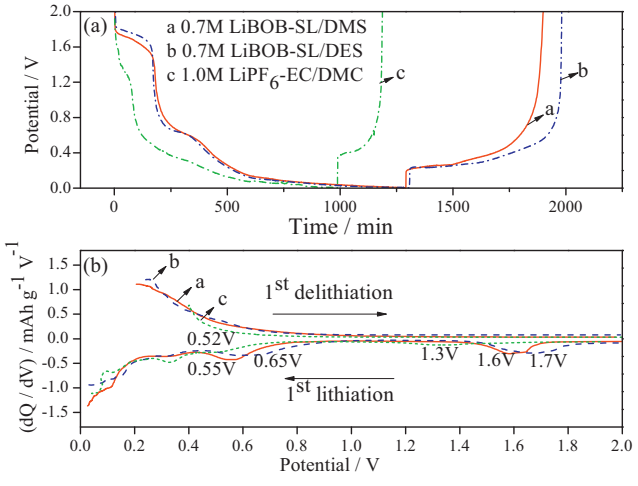

Fig. 3. (a) The first charge and discharge curves and (b) Differential capacity plots of Li/MCMB cells with different electrolytes.

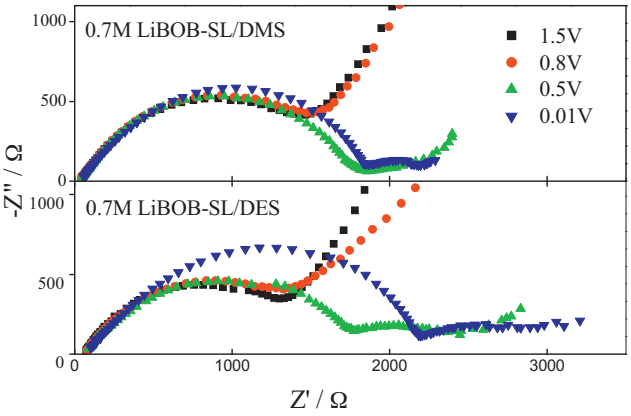

Fig. 4. The impedance spectra of the first cycle of Li/MCMB half-cells with two kinds of LiBOB-based electrolytes, respectively.

3.4. Impedance characteristics of Li/MCMB cells in different cycle numbers

Fig. 4 shows the impedance spectra of the first cycle of Li/MCMB half-cells with two kinds of LiBOB-based electrolytes, respectively. At the potential of 1.5 V, each of the impedance spectra shows a single high-frequency arc and a straight sloping line in the low frequency region. The existence of a single high-frequency arc implies the formation of the preliminary unstable SEI layer arose from the reduction of BOB anion [15,16]. No significant chemical reaction takes place in the potential range from 1.5 V to 0.8 V, because the impedance spectra are nearly unchanged at the potential of 0.8 V compared to that at 1.5 V. Each of the EIS spectra is composed of two partially overlapped semicircles in the range from the high to medium frequency and a short spike in the low frequency range at the potential of 0.5 V or 0.01 V. Each of the high-frequency arcs becomes larger gradually with the decreasing of potential, respectively. It implies the continuous formation of a dense and stable SEI layer, which is arose from the reduction of both electrolyte components and surface chemical groups of graphite [10,17]. The medium-frequency arcs arise from the charge-transfer resistances. Each of them also respectively becomes larger gradually with the decreasing of potential, which implies the process of lithiation.

Fig. 5 shows the impedance spectra of the cells with different electrolytes at different cycle numbers (1st cycle, 10th cycle, 30th cycle and 50th cycle). The impedance measurements were taken at the fully lithiated state of 0.003 V (the cut-off voltage of the discharge process for Li/MCMB cell). With the increase of circulation numbers, there are some obvious impedance differences for three kinds of electrolytes. Impedance of the cell with

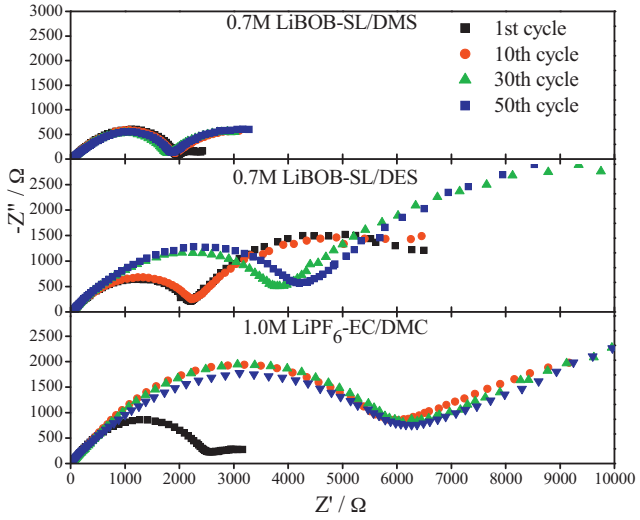

Fig. 5. The EIS spectra of Li/MCMB half-cells respectively with three kinds of electrolytes at deferent cycle numbers.

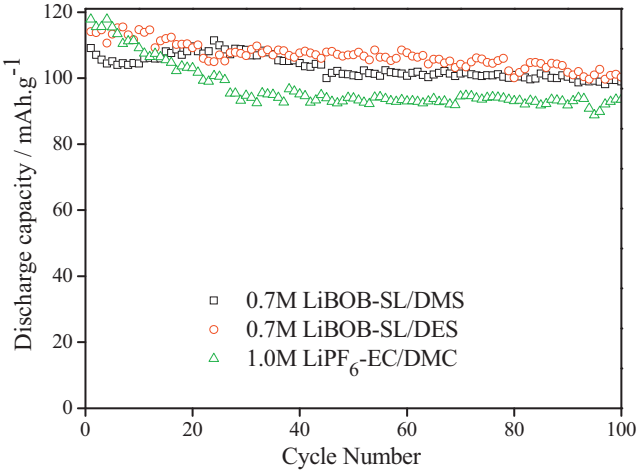

Fig. 6. The discharge capacity retentions of the $LiFePO_4$/Li cells with 0.5 C discharge rate at room temperature.

LiBOB-SL/DMS electrolyte is almost invariable. Impedance trend of the cell with LiBOB-SL/DES electrolyte changes little. However, impedance of the cell with $LiPF_6$-EC/DMC electrolyte is significantly enlarged. That is to say, the formation of $LiPF_6$-based SEI layer would not effectively stabilize the negative electrode to inhibit the further decomposition of electrolyte on the negative electrode, when compared to LiBOB-based electrolytes. Since the cycle life, discharge capacity, and safety performance of lithium ion batteries are highly depended on the performance of the SEI layer, therefore, LiBOB-based electrolytes, especially for LiBOB-SL/DMS electrolyte, can be considered as the promising candidate for lithium-ion batteries electrolyte compared with $LiPF_6$-EC/DMC electrolyte.

As shown in Fig. 5, in the impedance spectra at any cycle numbers in our test, every radius of the first semicircle for cells with LiBOB-based electrolytes is respectively smaller than that of the cell with $LiPF_6$-based electrolyte. It indicates that the resistance of the interface film of the cell containing the LiBOB electrolyte is much better than that of the cell containing the $LiPF_6$-based electrolyte. Compared with the cell with traditional electrolyte based on LiBOB, whose resistance of the interface film is almost two times of that of $LiPF_6$-based cell [19,20], these novel electrolytes are very attractive.

The possible mechanism of impedance reduction benefits from the rich sulfurous compounds in SEI layer, which are better conductors of Li^+ ions than analogical carbonates. Both of the sulfites DMS and DES are easy to decompose into Li_2SO_3, $(CH_2OSO_2Li)_2$ and so on, so each of these sulfites could significantly positively influence the electrochemical behavior of carbon anode [9]. But impedance of the cell based on each of these sulfites is still much bigger than $LiPF_6$-based cell [9], which indicates that SL is an essential cause of the obvious impedance reduction for Li/MCMB cells. Species and quantities of sulfurous compounds are increased remarkably, by the decomposition of SL into SO_2, Li_2SO_3, $((CH_2)_4SO_2Li)_2$ and so on. The complete results will be reported in detail in due course.

3.5. Cycle performances of $LiFePO_4$/Li cells

The capacity loss of a lithium ion battery along with cycle is mainly caused by both the cyclable lithium loss resulted from lithium-consuming SEI layer growth and the rate capability loss mostly due to the rise of interfacial resistance [21,22]. Fig. 6 shows the cycling performances of $LiFePO_4$/Li half cells with three kinds of electrolytes with 0.5 C discharge rate at room temperature, respectively. All cells are tested for 100 cycles. Although the $LiPF_6$-based cell has the highest discharge capacity density (117.8 mAh g^{-1}) in the first cycle, its average capacity density is lower than that of LiBOB-based cell. For example, in the first 100 cycles, the average capacity density of the cell with $LiPF_6$-EC/DMC electrolyte was calculated to be 97.0 mAh g^{-1}, lower than that of the cell with LiBOB-SL/DMS electrolyte (103.2 mAh g^{-1}). That is because, in the first 30 cycles, the cell with $LiPF_6$-EC/DMC electrolyte shows obvious fading capacity, while both of the cells with LiBOB-based electrolytes maintain constant capacities. After 100 cycles, the capacity retention efficiency of the cell respectively with LiBOB-SL/DMS and LiBOB-SL/DES electrolyte was found to be 90.7% and 87.9%, which are both higher than that of the cell with $LiPF_6$-EC/DMC electrolyte (79.3%). It infers that each of these novel electrolytes has significant factors in controlling the property of the capacity loss for lithium ion batteries.

Fig. 7 shows charge–discharge curves of $LiFePO_4$/Li cells respectively with three kinds of electrolytes in the 30th cycle with 0.5 C discharge rate at room temperature. It can be observed that every LiBOB-based cell shows obvious charge–discharge plateau, and small difference value of charge–discharge voltage. For example, the difference value of charge–discharge voltage of the cell with LiBOB-SL/DMS electrolyte was found to be only 0.12 V, which is much smaller than that of the cell with $LiPF_6$-EC/DMC (about 0.4 V),

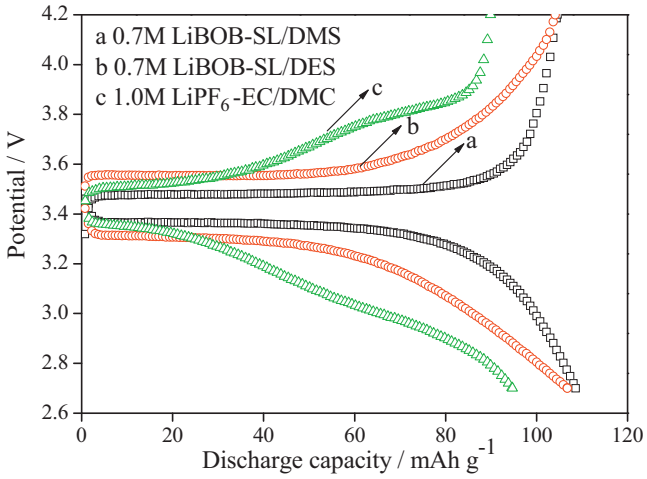

Fig. 7. The charge–discharge curves of $LiFePO_4$/Li cells with different electrolytes in the 30th cycle at room temperature, with 0.5 C discharge rate.

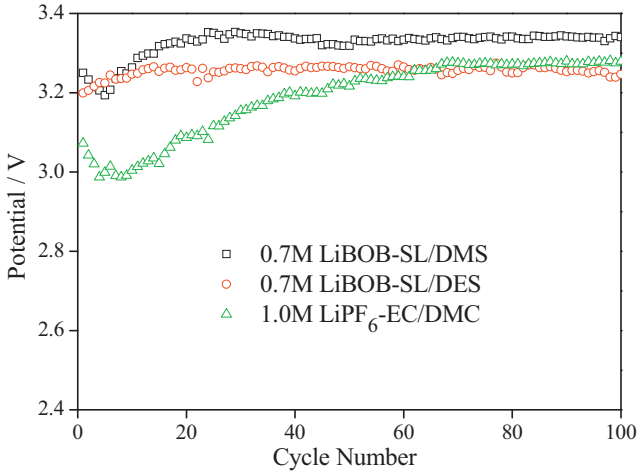

Fig. 8. Mean voltages of the $LiFePO_4$/Li cells with different electrolytes with 0.5 C discharge rate at room temperature.

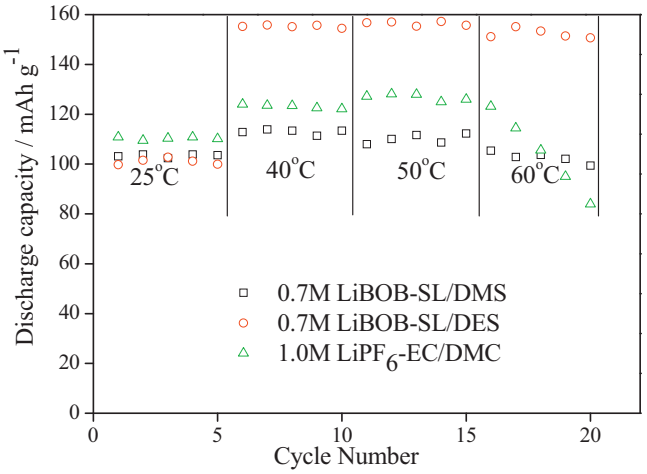

Fig. 10. The discharge capacities of $LiFePO_4$/Li cells at different temperature with 0.5 C discharge rate.

indicating a small polarization potential and a good cycle performance.

Mean voltage, the voltage at half time of the cells' running, reflects how long the cells can run under normal work voltage. From Fig. 8, it is obvious that the cell with LiBOB-SL/DMS or LiBOB-SL/DES electrolyte has higher mean voltage than that of the cell with $LiPF_6$-EC/DMC electrolyte. For example, in the first 30 cycles, the average mean voltages of the cell with LiBOB-SL/DMS or LiBOB-SL/DES electrolyte respectively was calculated to be 3.35 V or 3.26 V, while the cell with $LiPF_6$-EC/DMC electrolyte was found to be only 3.16 V. The reason may be due to the fact that $LiPF_6$-based cells have higher electrode polarization resistance than that of LiBOB-based cells, and hinder the de-intercalation and re-intercalation of Li^+ ions, as shown in Fig. 7.

3.6. *Capacity retentions of $LiFePO_4$/Li cells with different discharge rates or at different temperatures*

The discharge capacities of $LiFePO_4$/Li cells with LiBOB-SL/DMS, LiBOB-SL/DES or $LiPF_6$-EC/DMC electrolytes are respectively tested with various current densities at room temperature (Fig. 9). With the increase of the discharge rate, the discharge capacity decreases owing to the increased current which results in a quick increase of polarization resistance and decrease of the voltage. Unfortunately, in our experiment, the cut-off voltage was still set at 2.7 V, at which the discharge is not completed owing to inadequate utilization of the active ingredients. When compared with two different salts cells, all the cells have similar current discharge capability retentions. For example, when the cell discharges with 2 C, cells with these three kinds of electrolytes respectively have about 51%, 53% and 56% capacity retentions, compared to discharge with 0.5 C.

Fig. 10 summarizes the capacity retentions of $LiFePO_4$/Li cells with 0.5 C discharge rate at the temperature of 25 °C, 40 °C, 50 °C or 60 °C. For the cell with LiBOB-SL/DES electrolyte, the discharge capacities obviously increase as temperature rises. On one hand, it benefits from the reduction of resistance at extraction or insertion of Li^+ ions at high temperature. On the other hand, it benefits from more sufficient utilization of active ingredients by decreasing of polarization resistance. The similar characters exist in the cell with LiBOB-SL/DMS electrolyte, though it is not as obvious as the one with LiBOB-SL/DES electrolyte. But when temperature reaches 60 °C, abnormal case exists in $LiPF_6$-based cell that the discharge capacity starts to decrease rapidly. Besides, from experimental results we found that only the LiBOB-based cells could be approxi-

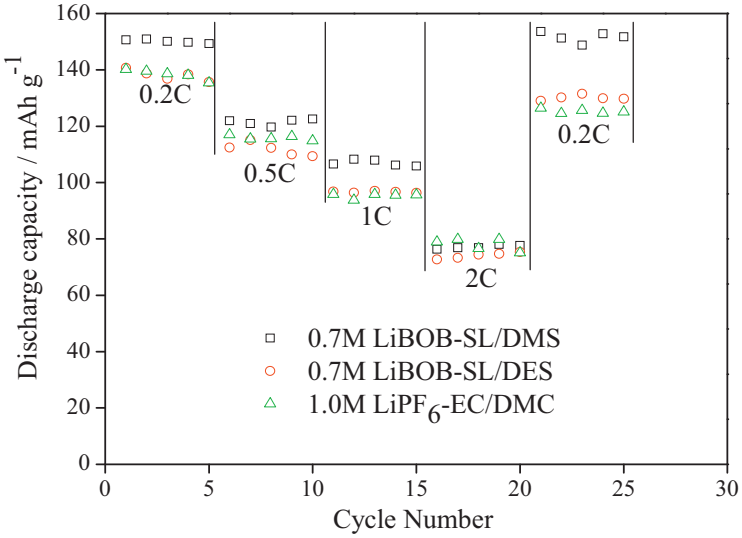

Fig. 9. The discharge capacities of the $LiFePO_4$/Li cells with different discharge rates at room temperature.

mate completely recovered when cells continued to run cycle after discharging at 60 °C. It means that LiBOB-based cells are more stable than $LiPF_6$-based cell at high temperature. The reason may be due to the fact that $LiPF_6$-based cell is damaged by the decomposition of $LiPF_6$ at 60 °C.

4. Conclusion

LiBOB is a promising salt for lithium ion batteries owing to its unique characteristics. Sulfolane and organic sulfites are promising solvents to exert the electrochemical performance of LiBOB. In this work, the electrochemical performances of two kinds of novel electrolytes, LiBOB-SL/DMS and LiBOB-SL/DES, were investigated. Both of their oxidation potentials are higher than 5.5 V, suggesting that these two kinds of novel electrolytes would be alternative electrolytes for 5 V high-voltage lithium ion batteries. Though both of their conductivities are lower than that of $LiPF_6$-EC/DMC electrolyte, they still show many excellent characters. When used in Li/MCMB cells, these two kinds of novel electrolytes exhibit not only excellent film-forming characteristics, but also low impedances of the interface films. Besides, when used in $LiFePO_4$/Li cells, compared to the cell with $LiPF_6$-EC/DMC electrolyte, each of the LiBOB-based electrolytes exhibits several advantages, such as more stable cycle performance even at elevated temperature, and higher mean voltage. It is suggested that both of the LiBOB-SL/DMS and LiBOB-SL/DES electrolytes are excellent candidate electrolytes for lithium ion batteries.

Acknowledgements

This work was supported by Science and Technology Planning Project of Gansu Province (No. 110RJYA056), the Scientific Research & Development Fund of Lanzhou University of Technology (No. SB05200903), Branchy Tamarisk Development Program for Young Teachers of Lanzhou University of Technology (No. Q201105) and the Natural Science Foundation of China (No. 20961004).

References

[1] S.E. Sloop, J.K. Pugh, S. Wang, J.B. Kerr, K. Kinoshita, Electrochem. Solid-State Lett. 4 (2001) A42–A44.
[2] K. Araki, N. Sato, J. Power Sources 124 (2003) 124–132.
[3] H.H. Lee, C.C. Wan, Y.Y. Wang, J. Elecrochem. Soc. 151 (2004) A542–A547.
[4] W. Xu, C.A. Angell, Electrochem. Solid-State Lett. 4 (2001) E1–E4.
[5] K. Xu, S.S. Zhang, T.R. Jow, W. Xu, C.A. Angell, Electrochem. Solid-State Lett. 5 (2002) A26–A29.
[6] K. Xu, S.S. Zhang, T.R. Jow, Electrochem. Solid-State Lett. 6 (2003) A117–A120.
[7] J.C. Panitz, U. Wietelmann, M. Wachtler, S. Strobele, M. Wohlfahrt-Mehrens, J. Power Sources 153 (2006) 396–401.
[8] M. Wachtler, M. Wohlfahrt-Mehrens, S. Ströbele, J.C. Panitz, U. Wietelmann, J. Appl. Electrochem. 36 (2006) 1199–1206.
[9] P. Ping, Q.S. Wang, J.H. Sun, X.Y. Feng, C.H. Chen, J. Power Sources 196 (2011) 776–783.
[10] S.S. Zhang, J. Power Sources 163 (2007) 713–718.
[11] Y. Watanabe, S.I. Kinoshita, S. Wada, K. Hoshino, H. Morimoto, S.I. Tobishima, J. Power Sources 179 (2008) 770–779.
[12] B.T. Yu, W.H. Qiu, F.S. Li, G.X. Xu, Electrochem. Solid-State Lett. 9 (2006) A1–A4.
[13] S.Y. Li, P.H. Ma, S.T. Song, Q.D. Ren, Russ. J. Electrochem. 44 (2008) 1144–1148.
[14] B.T. Yu, W.H. Qiu, F.S. Li, L. Cheng, J. Power Sources 158 (2006) 1373–1378.
[15] S.S. Zhang, M.S. Ding, K. Xu, J. Allen, T.R. Jow, Electrochem. Solid-State Lett. 4 (2001) A206–A208.
[16] E. Peled, C. Menachem, D. Bar-Tow, A. Melman, J. Electrochem. Soc. 143 (1996) L4–L7.
[17] S.S. Zhang, K. Xu, T.R. Jow, Electrochim. Acta 51 (2006) 1636–1640.
[18] S.S. Zhang, K. Xu, T.R. Jow, J. Power Sources 143 (2005) 197–202.
[19] D.P. Abraham, M.M. Furczon, S.H.K.D.W. Dees, A.N. Jansen, J. Power Sources 180 (2008) 612–620.
[20] M.Q. Li, M.Z. Qu, X.Y. He, Z.L. Yu, Electrochim. Acta 54 (2009) 4506–4513.
[21] M. Safari, M. Morcrette, A. Teyssot, C. Delacourt, J. Electrochem. Soc. 156 (2009) A145–A153.
[22] C.H. Huang, K.L. Huang, H.Y. Wang, S.Q. Liu, Y.Q. Zeng, Electrochem. Solid-State Lett. 15 (2011) 1987–1995.